Photonically enabled agile rf waveform generation by optical comb shifting

Christopher M. Long,* Daniel E. Leaird, and Andrew M. Weiner

School of Electrical and Computer Engineering, Purdue University, 465 Northwestern Avenue, West Lafayette, Indiana 47907-2035, USA

**Corresponding author: long25@purdue.edu*

Received August 19, 2010; revised October 7, 2010; accepted October 12, 2010; posted October 28, 2010 (Doc. ID 133647); published November 18, 2010

We present a photonically enabled rf arbitrary waveform generator that can rapidly switch between two output waveforms. This method is based on line-by-line shaping of an optical comb and then converting the optical pulses to rf waveforms with a fast photodetector. It uses a single diode laser as the optical source and selects different patterns preprogrammed into an optical pulse shaper by shifting the laser frequency. We demonstrate minimum update delay times of 0.45 ns. © 2010 Optical Society of America

OCIS codes: 320.5540, 060.5060, 060.5625, 070.6110.

Optical pulse shaping based on Fourier imaging is a powerful tool that can be used to generate complex optical waveforms [1,2]. Recent work has demonstrated programmable rf arbitrary waveform generation (RF-AWG) by converting optical pulses into electrical waveforms [3–5]. This method is limited by the slow response times of programmable optical pulse shapers, but a faster response would be a benefit for many applications, such as synthesis of millimeter power spectra [6], ultra-wideband communications [7], and photonically enabled rf filtering [8]. The update delay may be substantially improved by preprogramming multiple waveforms into the pulse shaper then selecting the desired waveform by manipulating the optical comb input. In one example [9], a rapid update was achieved by switching between two cw lasers that operated at different wavelengths. The switched signal was spectrally broadened into a comb by strong periodic modulation and coupled into a line-by-line pulse shaper [2], where the signal associated with each laser sampled a pattern on a separate region of the mask and therefore produced a different output waveform. Alternatively, it has been proposed to employ patterns that are interleaved on a mask, and then achieving optical waveform update by shifting the laser frequency by a small amount [10]. Here for the first time, we implement the method proposed in [10] using a directly modulated diode laser and demonstrate RF-AWG with waveform update delays as short as 0.45 ns.

Our experimental setup is similar to the work presented in [9] but replaces the pair of lasers and the pair of external intensity modulators with a single frequency-modulated diode laser, shown in Fig. 1. An electronic pulse source provides the high-speed square-wave signal that causes the lasing mode to shift to new frequencies. A spectrally flat, 20.4 GHz optical comb is generated and then passed through a line-by-line pulse shaper. In our pulse shaper, the optical comb is spatially dispersed using a diffraction grating, and then its individual spectral components are resolved in the focal plane of a $4F$ imaging system. Shaping is performed by a programmable array of 128 liquid crystal modulator pixels that can independently adjust the phase and attenuation of the incident light with a stated response time of 70 ms. Each pixel is 100 μm in width, corresponding to a spectral resolution of 5.1 GHz. Pixels are programmed in pairs, giving an effective minimum spectral resolution of 10.2 GHz per "superpixel." For each 20.4 GHz comb spacing, there are two distinct superpixels, corresponding to two different waveforms selectable based on the laser frequency. The shaped pulses are converted to an electrical signal by a high-speed (60 GHz) photodetector and viewed using a 50 GHz sampling oscilloscope.

Frequency modulation of the laser creates an output with a spectral envelope defined by the shape and amplitude of the modulation function [11]. Here, the modulation function is a square wave that produces a spectrum with optical power concentrated at frequencies $\nu \pm \Delta F$, where ν is the carrier frequency and ΔF is set by the amplitude of the modulation function. Circuit parasitics and charge carrier lifetimes distort the modulation signal but are mitigated by adding preemphasis to the input signal. With preemphasis, the modulation signal overshoots its intended value for a brief time before returning to the steady-state value. This is achieved by setting the pulse generator to produce a bipolar signal and combining the output with a delayed and attenuated version of the complementary output. For a short time (the added delay), the two signals add to produce a preemphasis signal, but for the rest of the period, the signals subtract to produce a nonzero steady-state signal.

This system uses a commercially available tunable DBR laser with a passive phase-tuning section (Oclaro iTLA TL5000), chosen because of the strong, current-based frequency modulation associated with DBR lasers

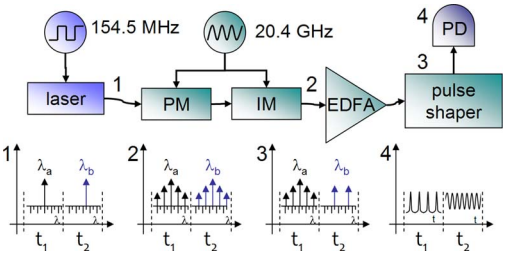

Fig. 1. (Color online) Schematic of experimental setup: PM, phase modulator; IM, intensity modulator; EDFA, erbium-doped fiber amplifier, and PD: photodiode. Bottom row, signal at various stages: 1, time-multiplexed wavelength generation, 2, combs, 3, shaped combs, and 4, rf waveforms.

[12]. Injecting small electrical currents into the phase-tuning section will produce strong frequency modulation with minimal thermal chirping. Past research has already demonstrated fast interchannel frequency hopping of a few nanoseconds with tunable DBR lasers [13], which could greatly expand the waveform generation abilities of this system over our previous effort [9]. In this work, however, we operate the laser with a reduced magnitude of frequency modulation within a single telecommunications channel, relaxing the electronic control requirements and reducing transition times to subnanosecond scales.

The laser is biased such that the carrier frequency is aligned to the edges of two superpixels in the pulse shaper mask. Frequency modulation is added to the laser, while the spectral shape is monitored on a spectrum analyzer. It is found that a 154.5 MHz square wave (that is, the comb repetition frequency divided by 132) of ±35 mV will produce modulation of ±2 GHz. We then use a pre-emphasis value of ±118 mV for 200 ps to generate the desired spectrum shown in Fig. 2(a). The external modulators produce an optical comb with five lines of similar power levels [Fig. 2(b)] that are modified by the pulse shaper [Fig. 2(c)]. In Fig. 2(c), the shaper is programmed to pass two spectral components from each half of the comb and attenuate the others. During the first half of the waveform, the carrier and first-order sideband of the longer-wavelength comb are mixed, producing the 20.4 GHz sinusoid shown in Fig. 2(d). During the second half of the waveform, the carrier and second-order sideband of the shorter-wavelength comb are mixed, producing the 40.8 GHz sinusoid shown in Fig. 2(e). The slight asymmetry seen in the 20.4 GHz waveform is due to unintentional contributions from the other spectral lines.

Actualized setups of cascaded intensity and phase modulators produce an optical comb in which the relative phase between adjacent spectral components varies rapidly with frequency. The first step in creating complex waveforms is to use the pulse shaper to adjust the spectrum so that the relative phase between the comb lines is 0, producing the transform-limited optical pulses shown in Fig. 3(c). The pulses possess a 20.4 GHz repetition frequency with a pulse width of 11.5 ps. In Fig. 3(a), all spectral components are allowed to pass through the pulse shaper, and the waveform amplitude is essentially constant in time. Figure 3(b) shows two complementary cases where only half of the dual comb is allowed to pass through the pulse shaper. It is seen that each half of the waveform has an envelope that is due to the laser spot sliding across one pixel to the next, producing a finite transition time between waveforms that is linked to our ability to produce square-wave modulation with sharp transitions. With improved modulation conditions, we achieved a minimum 10/90 transition time of 0.45 ns [Fig. 3(d)].

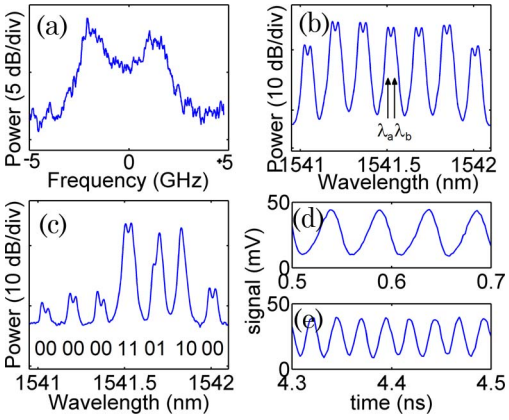

Fig. 2. (Color online) (a) Modulated laser spectrum measured by heterodyne detection. Pulse shaper output showing (b) full and (c) shaped spectra measured by an optical spectrum analyzer with 0.01 nm resolution. The programmed transmission function is displayed as zeros and ones. Time-multiplexed rf waveforms: sinusoids at (d) 20.4 and (e) 40.8 GHz.

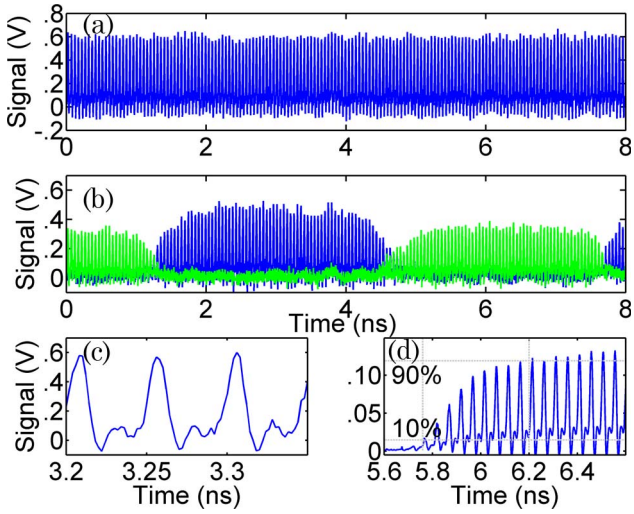

Fig. 3. (Color online) Waveforms composed of transform-limited pulses. (a) Output when the pulse shaper transmits all lines or (b) only half of the dual comb. Waveform during (c) steady state and (d) transition.

An example of switching between different rf waveforms with an approximately constant amplitude is presented in Fig. 4. The waveform changes from a pulse train during the first half-cycle into a 40.8 GHz sinusoid during the second half, similar to the waveforms shown in Figs. 3(c) and 2(e), respectively. The spectrogram in Fig. 4(b) is generated by calculating the Fourier transform of the signal within a sliding 200 ps Gaussian window. The pulse train produces the expected power at

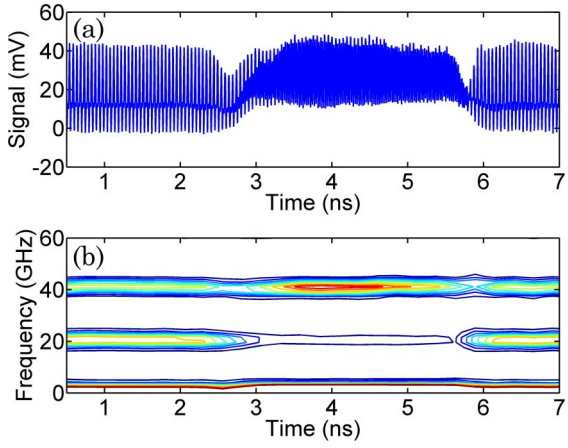

Fig. 4. (Color online) (a) Detected signal and (b) spectrogram for a waveform switching from a pulse train to a 40.8 GHz sinusoid. Contour lines indicate a 10% increase in signal.

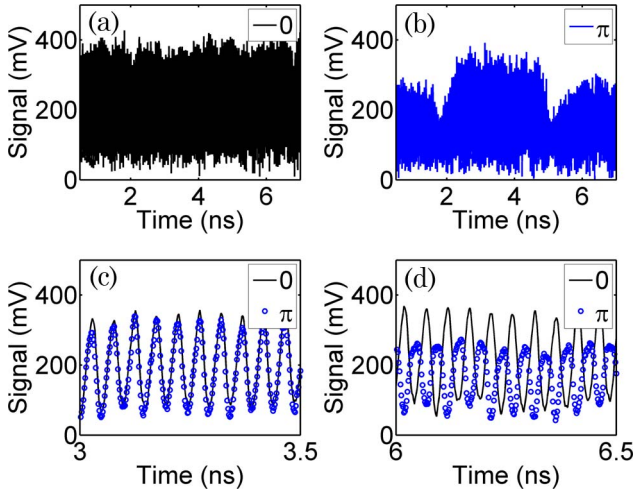

Fig. 5. (Color online) Sinusoid with rapid phase shift of π radians. Full waveform with both halves (a) in phase and (b) out of phase. Details of waveform for (c) in-phase and (d) out-of-phase conditions.

harmonics of the comb repetition frequency, but they are limited by the electrical bandwidth of the detection system. The other half of the waveform shows the 20.4 GHz harmonic suppressed to less than 10% but still present due to the finite contrast ratio of the pulse shaper.

An example showing a waveform with rapid phase change is shown in Fig. 5. Both halves of the waveform are composed of 20.4 GHz sinusoids. In one case, however, the pulse shaper introduces a phase of π to the first sideband of the optical comb, which, in turn, adds a phase shift of π to the rf output. The π-shifted waveform in Fig. 5(b) shows decreased amplitude, which can be attributed to the limited modulation depth of the tunable laser (± 2 GHz). Even though the laser spot is steered primarily onto a single superpixel, the tail of the spot impinges on the boundary between superpixels, leading to diffractive loss in the pulse shaper that disappears when both pixels are programmed the same.

In summary, we demonstrate a new method for rapidly switching between two rf waveforms that is photonically enabled and relies on shifting the optical carrier in an optical pulse shaper. By frequency modulating a laser, we select different patterns that are preprogrammed in our pulse shaper, resulting in two time-multiplexed waveforms that can be toggled as fast as 0.45 ns. Here, we present electrical pulses and sinusoids, but more complex shapes are possible with faster photodetectors or higher resolution pulse shapers. This method presents a scalable solution for rapidly switching between many pairs of output waveforms, but it ultimately requires a laser that has been optimized for high-speed frequency modulation [14] to achieve its full potential.

The authors are grateful to Andrew Christianson and William Chappell at Purdue University for help in the microwave design aspects of this project. This project was supported in part by the Naval Postgraduate School under grant N00244-09-1-0068 under the National Security Science and Engineering Faculty Fellowship program. Any opinions, findings, and conclusions or recommendations expressed in this publication are those of the authors and do not necessarily reflect the views of the sponsors.

References

1. A. M. Weiner, Rev. Sci. Instrum. **71**, 1929 (2000).
2. Z. Jiang, C. B. Huang, D. E. Leaird, and A. M. Weiner, Nat. Photon. **1**, 463 (2007).
3. J. D. McKinney, D. E. Leaird, and A. M. Weiner, Opt. Lett. **27**, 1345 (2002).
4. J. Chou, Y. Han, and B. Jalali, IEEE Photon. Technol. Lett. **15**, 581 (2003).
5. P. J. Delfyett, S. Gee, M. T. Choi, H. Izadpanah, W. Lee, S. Ozharar, F. Quinlan, and T. Yilmaz, J. Lightwave Tech. **24**, 2701 (2006).
6. C. B. Huang, D. E. Leaird, and A. M. Weiner, IEEE Photon. Tech. Lett **21**, 1287 (2009).
7. I. S. Lin, J. D. McKinney, and A. M. Weiner, IEEE Microw. Wireless Compon. Lett. **15**, 226 (2005).
8. E. Hamidi, D. E. Leaird, and A. M. Weiner, IEEE Trans. Microw. Theory **58**, 1 (2010).
9. C. B. Huang, D. E. Leaird, and A. M. Weiner, Opt. Lett. **32**, 3242 (2007).
10. J. Caraquitena and J. Marti, Opt. Lett. **34**, 2084 (2009).
11. H. Olesen and G. Jacobsen, IEEE J. Quantum Electron. **18**, 2069 (1982).
12. S. Murata, I. Mito, and K. Kobayashi, IEEE J. Quantum Electron. **23**, 835 (1987).
13. J. E. Simsarian, M. C. Larson, H. E. Garrett, H. Xu, and T. A. Strand, IEEE Photon. Tech. Lett. **18**, 565 (2006).
14. M. Pantouvaki, C. C. Renaud, P. Cannard, M. J. Robertson, R. Gwilliam, and A. J. Seeds, IEEE J. Sel. Top. Quantum Electron. **13**, 1112 (2007).